

Finite Element Analysis of Rectangular Raft Foundation in Expansive Clay Soil

T.W.E. Adejumo^{1,*} and I. A. Ojetunde²

Department of Civil Engineering, Federal University of Technology, Minna, Niger State, Nigeria
¹adejumo.taiye@futminna.edu.ng, ²isaiahoje@gmail.com, * Corresponding author

ABSTRACT

Raft foundation is a combined footing that covers the entire area beneath a structure and supports all walls and columns. This paper presents the analysis of raft foundation in an expansive clay soil. Plaxis 3D computer software was used for the analysis. Deformations of the soil and the raft foundation at the initial, excavation and Loading stages were analyzed. The deformation of the clay was higher at the excavation stage with a value of 4.96×10^{-3} m, compared with 722.57×10^{-6} m recorded at the initial stage. With the introduction of modelled raft, the total deformation at this stage reduced to 712.22×10^{-6} m, with the raft serving as both stiffener and brace, plus loading rate efficiency of 96.2%. Under the same pressure, the deformation obtained using the classical Mohr-Coulomb model is higher than the one obtained using the Finite Element Analysis. Finite Element Analysis is therefore recommended for raft foundation analysis.

Keywords: *Finite element analysis, Expansive Clay Plaxis 3D, Raft foundation, Sensitive Clay soil*

1 INTRODUCTION

Raft foundation are sometimes referred to as raft footings (Jawad, 1998). They are formed by reinforced concrete slabs of uniform thickness that cover a wide area, often the entire footprint of the building (Jawad, 1998). Raft foundation are widely used in supporting structures for many reasons such as weak soil conditions or heavy column loads (Pusadkar and Bhatkar, 2013).

Clays are the finest grained soils. The upper limit on grain size is 0.002mm, but most of the clay particles will even be smaller (Johnson, 1969). Clay soil pose a great hazard in regions with pronounced wet and dry season. The annual cycle of wetting and drying causes clay soil to shrink and swell each year (Yenes *et al.*, 2012)

The use of Finite element procedures has gained wide application in engineering analysis (Kraskiewicz *et al.*, 2015). With its effectiveness, its use is expected to increase significantly in years to come. The procedures are employed extensively in the analysis of solids and structures (De-Weck and Kim, 2004) and of heat transfer and fluids, and indeed, finite element methods are useful in virtually every field of engineering analysis

Several works have been done on the analysis of deep and shallow foundation. Conte *et al.* (2013) investigated *Progressive failure analysis of shallow foundations on soils with strain-softening behaviour*. The work employed finite element approach in which a non-local elasto-visco-plastic constitutive model in conjunction with the Mohr–Coulomb yield function was incorporated. The model proposed prediction of the

response of strip footings resting on soils with strain-softening behaviour. This behaviour is simulated by reducing the strength parameters with increasing accumulated deviatoric plastic strain.

Al-Zaidee, Fadhil and Al-Kubaisi (2015) used finite element to modify Winkler model for raft foundation supported on dry granular soils and in an attempt to modify traditional Winkler model to take shear forces between adjacent soil prisms into account in computing subgrade reactions and bending moments in raft foundations, two finite element soil simulations was considered in their study and in the first model, Winkler simulation was adopted while in the second one soil mass was simulated with brick finite element.

SaadEldin and El-Helloty (2014), analysed raft foundation using PLAXIS programme to study the effect of opening position and different types of soil. They found that opening and type of soil have important effect on settlement of soil and moment of raft foundation.

With the recent increase in building collapse in many part of Nigeria, which has led to loss of lives and properties, which among other thing has been traced to structural, construction or member failure including foundation. The foundation failure on

expansive clay soil will be analysis using Plaxis 3D software.

2 RESEARCH METHODOLOGY

2.1 MATERIALS

2.1.1 Soil: The soil used in this study was collected using the disturbed sampling technique at depths of 0 meter, 1 meter and 1.5 meters from selected borrow pits in three locations around Talba farm sites, Minna, Niger state, Nigeria.

2.1.2 Plaxis 3D software: Finite element analysis was carried out using PLAXIS 3D 2013 software with correlated compatibility with Mohr-Coulomb model. All data necessary for the Mohr-Coulomb model were calculated and imputed. These parameters with their standard units are listed as: E: Modulus of elasticity [kN/m^2], ϕ : Angle of internal friction [$^\circ$]; ν : Poisson's ratio [-]; c: Cohesion [kN/m^2], ψ : Angle of dilatancy [$^\circ$]; γ_{sat} , γ_{unsat} : Saturated and Unsaturated unit weight respectively [kN/m^3].

2.2 METHODS

2.2.1 Index properties: Natural moisture content, specific gravity, particle size distribution or sieve analysis and Atterberg limits tests were conducted in accordance with tests procedures specified in BS 1377: 1990.

2.2.2 Compaction characteristics:

compaction of clay specimens was conducted in accordance with the guidelines specified in BS 1377 (1990) to compute the required parameters. The Reduced British Standard light (RBSL) compactive effort was used. The RBSL compaction is the energy resulting from 2.5 kg rammer falling through a height of 30 cm onto three layers, each receiving 25 blows.

2.2.3 Consolidated undrained triaxial test:

The CU test of samples was conducted in accordance with the procedure specified in BS, 1377: (1990). The treated specimens were prepared relative to OMC and compacted with RBSL compactive energy. the CU test was done using all round pressure of 50, 100 and 150 kN/m² on each of the specimen taken from the three layers having been moulded using the MDD and OMC from compaction test.



Plate 1: Consolidated undrained test of samples

2.3 Model Foundation Analysis

The analysis was conducted on a model raft foundation of 40 metres long, 20 metres wide and 1.5 metres deep. Six loads of 5000 kN were applied on the foundation, at 10 metres interval. Figure 1 shows the dimensions of the foundation and the positions where the loads were applied.

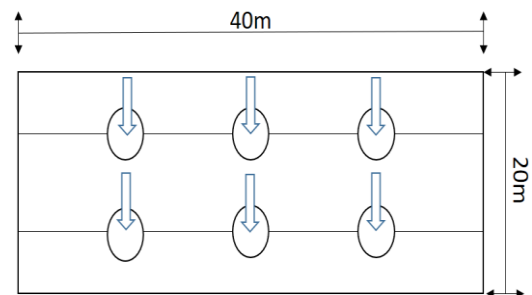


Figure 1: Loading points of modeled Raft Foundation

2.4 Constitutive Models

2.4.1 Mohr-Coulomb Model

Coulomb proposed the first plasticity model in soil mechanics. It is composed of two symmetrical lines in Mohr's plane (σ, τ), having an angle ϕ with the normal stresses axis, σ with the expression in equation (2.1):

$$F(\sigma_{ij}) = \sigma_1 - \sigma_3 - (\sigma_1 + \sigma_3) \sin \phi - 2c \cos \phi \leq 0 \quad (2.1)$$

Where:

σ_1 and σ_3 are the extreme main stresses

c is represents the soil cohesion,

ϕ is the internal friction angle in degree

In the space of main stresses ($\sigma_1, \sigma_2, \sigma_3$) the surface defined by function F is a pyramid

with hexagonal section having as axis the line $\sigma_1 = \sigma_2 = \sigma_3$.

The plastic potential defined as a function of the extreme main stresses is:

$$G(\sigma_{ij}) = \sigma_1 - \sigma_3 + (\sigma_1 + \sigma_3) \sin \varphi + \text{const} \quad (2.2)$$

Where:

φ is the dilatancy angle ($\varphi = \phi$ if it is an associated criterion).

The elasticity associated to the Mohr – Coulomb criterion is a linear Isotropic-Hooke type one. The criterion contains 5 mechanical parameters:

- i. E – elasticity modulus,
- ii. ν - Poisson’s coefficient: elastic parameters;
- iii. c, ϕ, ψ : plastic parameters.

3 RESULTS AND DISCUSSION

3.1 Variation of Index Properties of the soil with depths

The index properties of the soils are shown in Table 1. The fraction of soil samples passing through No 200 (75 μm) sieve for depth 0m, 1m and 1.5m are 68.57%, 70.73% and 71.27% respectively. The soils are classified A-7-5 (or CL), A-7-5(or CH) and A-7-6 (or CH) at 0m, 1.0m and 1.5m depth respectively according to AASHTO and USC classification systems respectively (AASHTO, 1986; ASTM, 1992). Therefore,

from this classification, the soil in all the test pits are clayey soils.

Table 1: Properties of the expansive clay

Properties (Average)	Layer	Layer	Layer
	A (0m)	B (1.0m)	C (1.5m)
Specific gravity of soil	2.73	2.58	2.75
Natural moisture content (%)	18.91	17.34	25.22
Atterberg Limits			
Liquid limit (%)	54.5	47.0	43.2
Plastic limit (%)	38.19	32.92	29.63
Shrinkage limit (%)	9.64	9.21	10.00
Plasticity index	16.31	14.08	13.57
% Passing BS No. 200 sieve	51.90	52.70	54.70
Classification			
USCS	CL	CH	CH
AASHTO	A-7-5	A-7-5	A-7-6

3.2 Consolidated Undrained Triaxial Test

The following are the results obtained from the test and computation of the results of samples collected from 0, 1.0 and 1.5 metres depths:

Table 2: Triaxial test results of samples at depth of 0m

Item	Quantity		
All round Pressure(kN/m ²)	50	100	150
Axial Deformation (mm)	400	600	525
Loading (N)	12	19	32

Table 3: Principal stresses of test samples at 0m

σ_3 (kN/m ²)	σ_2 (kN/m ²)	σ_1 (kN/m ²)
50	72	122
100	110	210
150	191	341

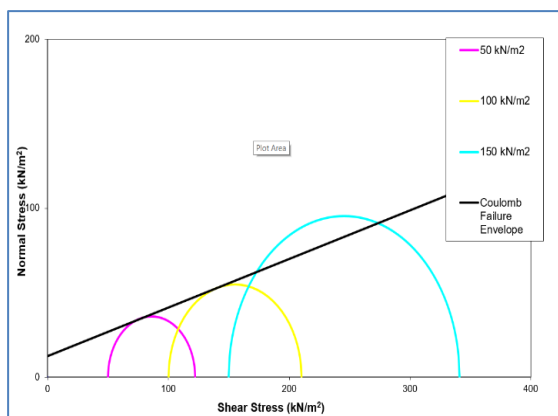


Figure 2: Mohr circle diagram samples at 1.0m

Table 4: Triaxial test results of samples at depth of 1.0m

Item	Quantity		
Principal stresses (kN/m ²)	50	100	150
Axial Deformation (mm)	400	525	425
Loading (N)	11.2	17	19.8

Table 5: Principal stresses of test samples at 1.0m

σ_3 (kN/m ²)	σ_2 (kN/m ²)	σ_1 (kN/m ²)
50	67	117
100	100	200
150	115	265

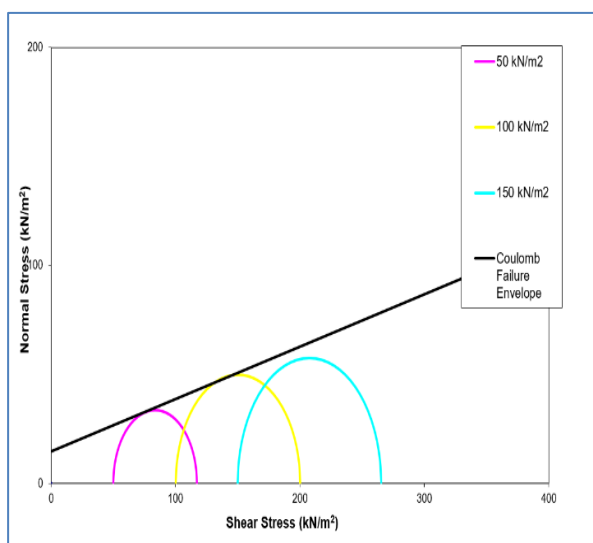


Figure 3: Mohr circle diagram for samples at 1.0m

Table 6: Triaxial test results of samples at depth of 1.5m

Item	Quantity		
Principal stresses (kN/m ²)	50	100	150
Axial Deformation (mm)	475	525	625
Loading (N)	13.2	20.1	30

Table 8: Principal stresses of test samples at 1.5m

σ_3 (kN/m ²)	σ_2 (kN/m ²)	σ_1 (kN/m ²)
50	78	128
100	118	218
150	173	323

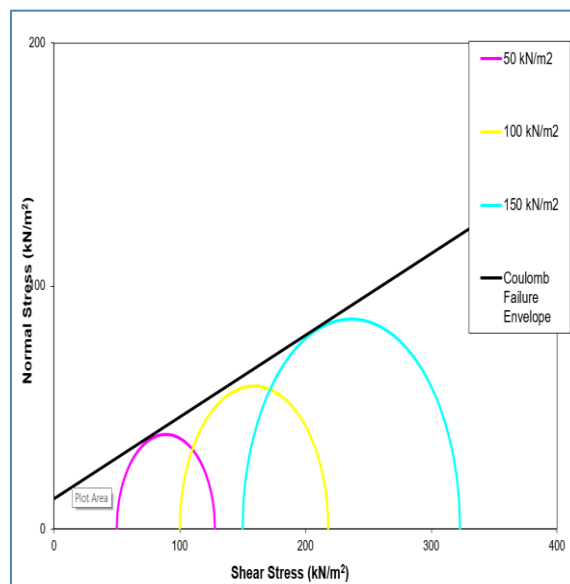


Figure 4: Mohr circle diagram of samples at 1.5m

Table 2: Summary of the input soil properties

Layer 1 (0 meter)	$\gamma_{sat} = 17.8 \text{ kN/m}^3$ $\gamma = 15.6 \text{ kN/m}^3$ $c = 12.3 \text{ kN/m}^2$ $\phi = 23^\circ$ $v = 0.25$ $E = 3000 \text{ kN/m}^2$ $\psi = 0$
Layer 2 (1.0m)	$\gamma_{sat} = 17.2 \text{ kN/m}^3$ $\gamma = 16.2 \text{ kN/m}^3$ $c = 14.7 \text{ kN/m}^2$ $\phi = 23^\circ$ $v = 0.23$ $E = 3000 \text{ kN/m}^2$ $\psi = 0$
Layer 3 (1.5m)	$\gamma_{sat} = 16.8 \text{ kN/m}^3$ $\gamma = 15.2 \text{ kN/m}^3$ $C = 12.3 \text{ kN/m}^2$ $\phi = 26^\circ$ $v = 0.23$ $E = 3000 \text{ kN/m}^2$ $\psi = 0$

Table 3: Input parameters of the raft foundation

Parameter	Value
Raft length	40m
Raft width	20m
Raft thickness	0.5m
Modulus of Elasticity (e)	$1.0 \times 10^7 \text{ kN/m}^2$
Poisson's ratio	0.3
Unit weight	24 kN/m^3

3.3 Deformation

3.3.1 Initial Stage Deformation

From the analysis, as shown in the interphase mesh in Plate II, the extreme deformation at the initial stage is $722.57 \times 10^{-6} \text{ m}$, which is lower than those of excavation and final stages. The load here is gradual and the soil around the foundation has still within the elastic state, with little or minimum distortion.

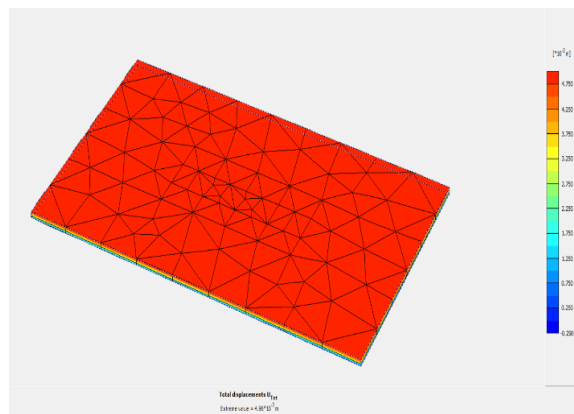


Plate II: Plaxis interphase at initial deformation stage

3.3.2 Excavation Stage Deformation

The increased deformation at the excavation stage is $4.96 \times 10^{-3} \text{ m}$. The deformation at this stage increased due to structural imbalance and particles phase distortion as well as destabilization resulting from displacement, remoulding and other disturbances during soil during excavation.

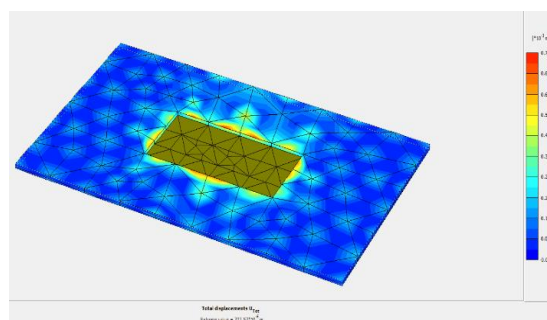


Plate III: Excavation stage deformation of the soil

3.3.3 Final Stage Deformation (Deformation caused by loading)

The extreme deformation at the final loading stage is $17.922 \times 10^{-3} \text{ m}$. However, with the introduction of model raft, the total deformation at this stage reduced to $712.22 \times 10^{-6} \text{ m}$, with the raft serving as both

stiffener and brace. In this case, the loading rate efficiency of raft foundation is 96.2%.

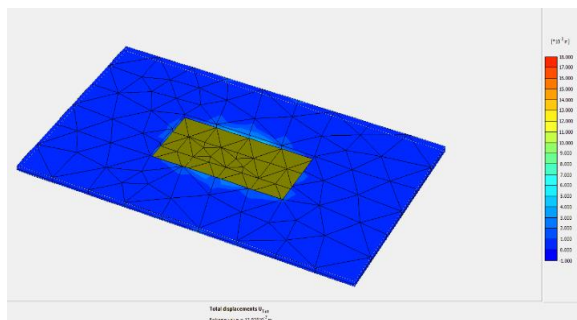


Plate IV: Final stage deformation of the soil samples

3.4 Comparison of Mohr-Coulomb model and Finite Element Method

Under the same threshold pressure, the deformation obtained using the classical Mohr-Coulomb model produced is higher than the one obtained using the finite element analysis. Under a threshold pressure of $\sigma = 320 \text{ kN/m}^2$, former produced a maximum deformation of $4.55 \times 10^{-3} \text{ m}$, while the latter produced a deformation $615.15 \times 10^{-6} \text{ m}$ respectively.

4 CONCLUSION

From the analysis of results of investigation of raft foundation in expansive clay, the following conclusions were drawn;

1. The deformation of the soft expansive clay was higher at the excavation stage than at

initial stage with values of $4.96 \times 10^{-3} \text{ m}$ and $722.57 \times 10^{-6} \text{ m}$ respectively.

2. The higher deformation at the initial stage was due to structural modification, phase distortion as well as destabilization resulting from displacement, remoulding and other disturbance of soil.

3. With the introduction of modelled raft, the total deformation at excavation stage reduced to $712.22 \times 10^{-6} \text{ m}$, with the raft serving as both stiffener and brace, with the loading rate efficiency of 96.2%.

4. Under the same threshold pressure, the deformation obtained using the classical Mohr-Coulomb model is higher than the one obtained using the Finite Element Analysis (FEA).

5. With the effectiveness of rectangular raft foundation in expansive clay, experimented in this study, deductions are made that, numerical analytical method namely, Finite Element Analysis is a useful tool in foundation analysis. Finite Element Analysis encoded in Plaxis or other software is therefore recommended for use in sites, where geotechnical investigations revealed availability of sensitive or expansive clay within or around the foundation recommended depth.

ACKNOWLEDGEMENTS

The authors wish to acknowledge the contributions of Lecturers, technologist, colleagues and other research fellows in Federal University of Technology, Minna.

REFERENCES

- AASHTO (1986). American Association of State Highway and Transport Officials. Standard Specifications for Transport Materials and Methods of Sampling and Testing. 14th Edition, AASHTO, Washington, D.C. United State of America.
- Conte, E., Donato, A., and Troncone, A. (2013). Progressive failure analysis of shallow foundations on soils with strain-softening behaviour. *Computers and Geotechnics* (54): 117–124.
- De-Weck, O. and Kim, I. Y. (2004). Finite Element Method. *Engineering Design and Rapid Prototyping*. Massachusetts Institute of Technology. 1-26.
- Jawad, T. A. (1998). Optimization of Raft Foundation Design. *MSc thesis*, University of Technology, Baghdad, Iraq.
- Kraskiewicz, C., Michalczyk R., Brezinski K. and Pludowska M. (2015). Finite Element modelling and design procedures for verifications of trackbed structure. *Procedia Engineering*, 111: 462 – 469.
- Pusadkar, S. S. and Bhatkar, T. (2013). Behaviour of Raft Foundation with Vertical Skirt Using Plaxis 2d. *International Journal of Engineering Research and Development* Volume 7(6): 20-24.
- Johnson L. D. (1969). Review of literature on expansive clay soils. *Miscellaneous paper S-69-24*. Army-Mrc, Vicksburg, Mississippi, United State of America.
- SaadEldin, M and El-Helloty, A. (2014). Effect of Opening on Behaviour of Raft Foundations Resting on Different Types of Sand Soil. *International Journal of Computer Applications*, 94(7): 132-140.
- Yenes, M., Nespereira J., Blanco J. A., Suarez M., Monterrubio S., and Iglesias, C. (2012). Shallow foundations on expansive soils: a case study of the El Viso Geotechnical Unit, Salamanca, Spain. *Bulletin of Eng Geol Environ*, 71:51–59.